NANO LETTERS

2003
Vol. 3, No. 11
1573−1576

The Small Heat Shock Protein Cage from *Methanococcus jannaschii* Is a Versatile Nanoscale Platform for Genetic and Chemical Modification

Michelle L. Flenniken,[†,||] Deborah A. Willits,[§,||,⊥] Susan Brumfield,[§,⊥] Mark J. Young,[*,†,§,||,⊥] and Trevor Douglas[*,‡,||,⊥]

Department of Microbiology, Department of Chemistry and Biochemistry, Department of Plant Sciences, Center for Bio-Inspired Nanomaterials, Thermal Biology Institute, Montana State University, Bozeman, Montana 59717

Received September 17, 2003

ABSTRACT

Nature has provided us with a range of reactive nanoscale platforms, in the form of protein cage architectures such as viral capsids and the cages of ferritin-like proteins. Protein cage architectures have clearly demarcated exterior, interior, and interface surfaces consisting of precisely located chemical functionalities. In the present work, we demonstrate that the small heat shock protein (MjHsp) cage from *Methanococcus jannaschii* is a new and versatile nanoscale platform whose exterior and interior surfaces are amenable to both genetic and chemical modification. Wild type and genetic mutants of the Hsp cage are shown to react with activated fluorescein molecules in a site specific manner. In addition, the 12 nm Hsp cage serves as a size constrained reaction vessel for the oxidative mineralization of iron, resulting in the formation of monodispersed 9 nm iron oxide nanoparticles. These results demonstrate the utility of the Hsp cage to serve as a nanoscale platform for the synthesis of both soft (organic) and hard (inorganic) materials.

A major goal of nanomaterials is the design and synthesis of multifunctional materials with precise molecular level control. One promising approach is the biomimetic synthesis of nanomaterials using organic assemblies as templates for directed fabrication.[1−3] Organic assemblies such as viral based protein cages and ferritin-like protein cages have been utilized as templates for constrained nanomaterials synthesis.[4−12] Protein cage architectures provide exterior, interior, and subunit interface surfaces on a nanoscale platform that can be genetically and chemically modified to impart function by design.[4−12] In the present work, we demonstrate that the small heat shock protein (MjHsp) from the hyperthermophilic archeaon, *Methanococcus jannaschii*, is a highly versatile cage-like structure whose exterior and interior surfaces are amenable to both genetic and chemical modification. Organic ligands were attached to the MjHsp cages in a site specific manner to the exterior and interior surfaces. In addition, the MjHsp cage was employed as a size constrained reaction vessel for the synthesis of inorganic materials. The demonstration of molecular level control in the MjHsp cage system illustrates its versatility as a multifunctional nanoscale platform. The ability to perform both inorganic and organic functionalization of this template indicates its potential applicability in nanomaterials[13] and biomedical[14] sciences.

The small heat shock protein (MjHsp) assembles into an empty 24 subunit cage with octahedral symmetry.[15−17] The assembled protein cage has an exterior diameter of 12 nm. Large, 3 nm diameter, pores at the 3-fold axes allow free exchange between the interior and bulk solution (Figure 1A).[15−17] In addition, the MjHsp cage is stable up to ∼70 °C[18] and in a pH range of 5−11. Each 16.5 kDa MjHsp monomer is composed of 147 amino acids but contains no endogenous cysteine residues.

The 3.2 Å resolution X-ray crystal structure provides the foundation for precisely defining the location of reactive groups on both the exterior and interior of the cage.[15−16] The endogenous cage provides spatially defined reactive groups, and through genetic engineering we are able to introduce additional reactive functional groups in a site specific manner. Naturally occurring lysines ($-NH_2$) are found both on the exterior surface (amino acid positions: 55, 65, 82, 110, 116, 123, 141, 142) and the interior surface (amino acid position 40) of the assembled MjHsp cage (Figure 1 A, B). To

* Corresponding authors. E-mail: tdouglas@chemistry.montana.edu; myoung@montana.edu
† Department of Microbiology.
‡ Department of Chemistry.
§ Department of Plant Sciences.
|| Center for Bio-Inspired Nanomaterials.
⊥ Thermal Biology Institute.

10.1021/nl034786l CCC: $25.00
Published on Web 10/11/2003

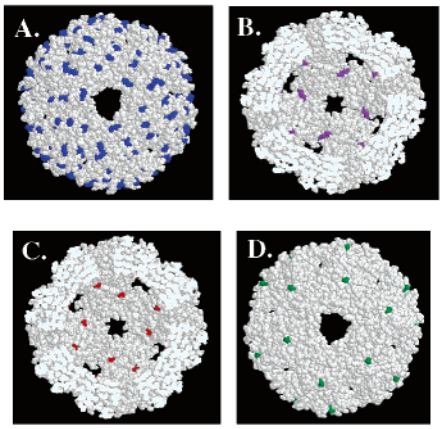

Figure 1. Space filling models of the 24 subunit MjHsp cages. (A) The exterior of the Hsp cage viewed along the 3-fold axis; lysines are colored blue. (B) The interior of the cage viewed along the 4-fold axis; lysines are colored purple. (C) The interior of the Hsp cage viewed along the 4-fold axis; the interior exposed amino acids, at subunit position 41, are colored red. In wtHsp position 41 is glycine, in a genetic mutant HspG41C position 41 is a cysteine. (D) The exterior of the cage viewed along the 3-fold axis; the externally exposed amino acid at subunit position 121 is colored green. In wtHsp position 121 is serine whereas in the genetic mutant HspS121C it is a cysteine.

engineer spatial selectivity, unique thiol functional groups were introduced via polymerase chain reaction (PCR) mediated site directed mutagenesis (Supporting Information). Glycine at position 41 on the interior surface was replaced with cysteine to generate the HspG41C mutant (Figure 1C). Similarly, serine at position 121 on the exterior surface was replaced by cysteine to generate HspS121C (Figure 1D). In brief, the gene encoding the small heat shock protein MjHsp16.5 was amplified by PCR, cloned into the pET-30a(+) plasmid (Novagen), and expressed in *E. coli*. The nucleic acid sequences encoding wild type, G41C, and S121C MjHsp clones were confirmed by DNA sequencing (Applied BioSystems). The MjHsp proteins were purified from *E. coli* where they self-assembled into the 24 subunit cages. These cages were purified to homogeneity as described in the Supporting Information. Recombinant protein cages were characterized by size exclusion chromatography (Superose 6, Amersham Pharmacia), dynamic light scattering (Brookhaven 90Plus), transmission electron microscopy (Leo 912 AB) (Figure 2), mass spectroscopy (Esquire3000, Bruker), and SDS polyacrylamide gel electrophoresis (SDS−PAGE) (Supporting Information).

To assess the reactivity of the introduced thiol and endogenous amine groups, the purified MjHsp protein cages were reacted with activated fluorescein. Specifically, fluorescein-5-maleimide (Fl-Mal) was used for reactions with thiols and 5-(and-6) carboxy-fluorescein-succinimidyl ester (5(6)-FAM) for reactions with amines.[19] For exposed thiol reactions, purified HspG41C cages (0.9 mg/mL, 54 μM) in HEPES buffer (100 mM, pH 6.5) were treated with tris(2-carboxyethyl)phosphine (TCEP) for 1 h at room temperature to ensure reduction of the thiol groups prior to labeling. Reactions to covalently bind 5(6)-FAM to the endogenous amine groups, on both the exterior and interior surfaces, were

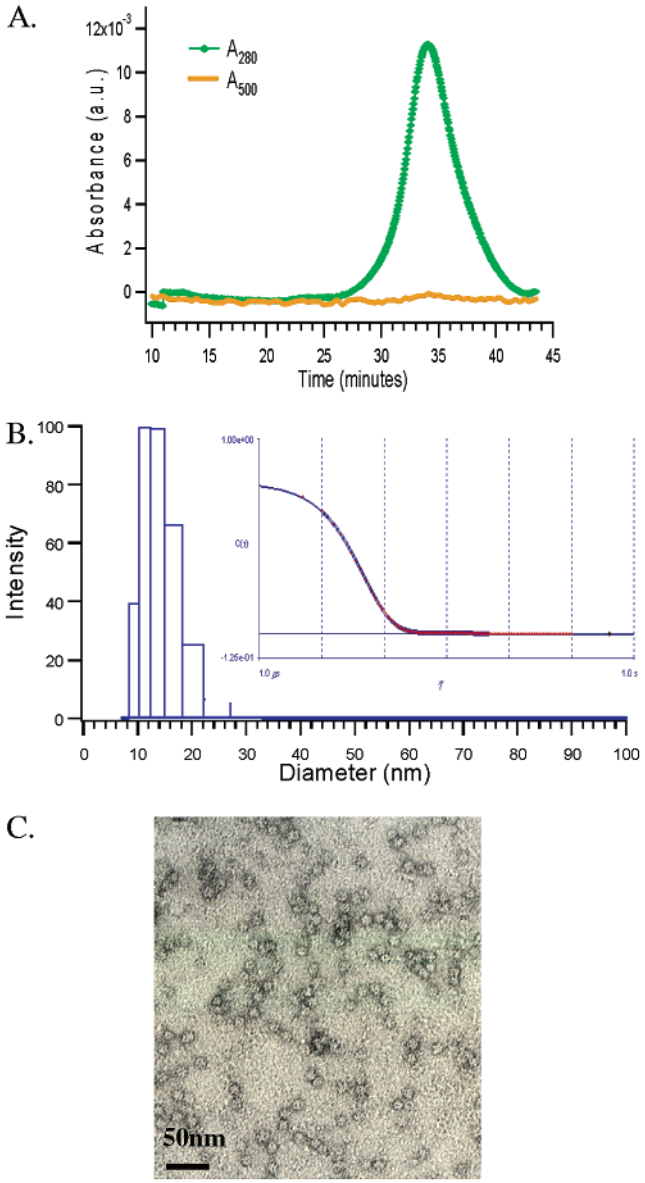

Figure 2. MjHsp cage characterization (A) Size exclusion chromatography absorbance profile. MjHsp elutes after 30 min (A280 nm). (B) Dynamic light scattering shows a mean diameter of 12.6 nm. The insert shows the correlation function of the raw data collected (red) and the fit of these data using a non-negatively constrained least squares (NNLS) analysis (blue). (C) Transmission electron microscopy of the 12 nm MjHsp cages negatively stained with uranyl acetate; 50 nm scale bar.

performed in 100 mM HEPES, pH 8.0. A range of fluorescein concentrations, from 0.06 to 28 molar equivalents per subunit, were reacted with the protein cages. The reactions proceeded at room temperature for 2 h with stirring, followed by incubation at 4 °C overnight. After the reactions, modified MjHsp was separated from unreacted fluorescein by size exclusion chromatography. Since fluorescein emission is pH sensitive,[19] 100 μL of Tris buffer (0.5 M, pH 8.5) was combined with column eluant (50 μL) prior to fluorescence analysis. The results showed selective labeling in HspG41C and HspS121C reactions with fluorescein-5-maleimide as compared to the wild type MjHsp control (Figure 3). HspG41C and HspS121C prereacted with iodoacetamide

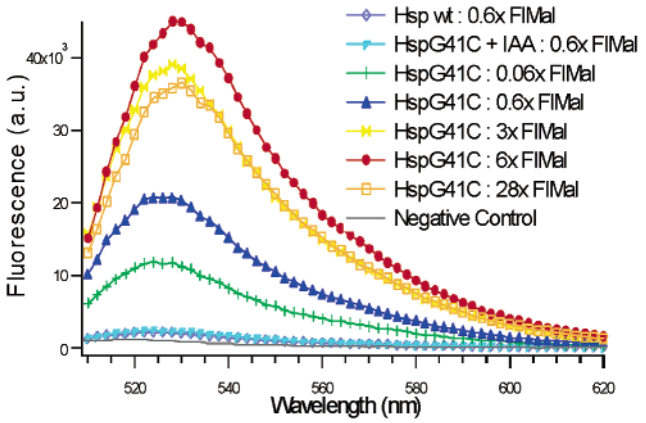

Figure 3. (A) Fluorescence emmision of the Hsp cages (either wild type (wt) or G41C) labeled with fluorescein-5-maleimide (FlMal). The fluorophore quantities listed are in molar equivalents of fluorophore per subunit. Protein free controls were performed at all fluorophore concentrations; one example is shown above (negative control = 3× fluorophore only). In each case, no free fluorophore was detected by fluorescence.

Table 1. Extent of MjHsp Labeling with Fluorophores (Fl-Mal = fluorescein-5-maleimide, FAM = 5-(and-6) carboxy-fluorescein-succinimidyl ester)[a]

Hsp cage	fluorophore conc[b]	# Fl-Mal/cage	# FAM/cage
WtHsp	0.6×	0.3	1
HspG41C+IAA; HspS121C+IAA	0.6×	0.6;0	N/A
HspG41C;S121C	0.06×	1;0	0
HspG41C;S121C	0.6×	3;0	1
HspG41C;S121C	3×	7;2	4
HspG41C;S121C	6×	24;5	8
HspG41C;S121C	28×	11;5	17

[a] The extent of labeling is shown by the number of fluorophore molecules covalently linked per cage. The Fl-Mal data indicate 100% labeling of the HspG41C reactive groups with 6× molar equivalents of fluorophore; compared to only 21% labeling of HspS121C. The decreased labeling of HspS121C might be due to reduced accessibility. Importantly, wtHsp, which lacks cysteines, does not show labeling with Fl-Mal. Control reactions, using HspG41C/HspS121C treated with iodoacetamide (IAA) to passivate reactive thiols prior to addition of Fl-Mal, showed low reactivity. [b] Fluorophore concentration is reported in molar equivalents per subunit.

(HspG41C/HspS121C + IAA), to passivate reactive thiols, served as additional control reactions. As expected, subsequent exposure to activated fluorescein did not result in covalent attachment of fluorescein; therefore, no fluorescence signal was observed in these reactions (Figure 3, Supporting Information). The number of fluorophore molecules covalently linked per MjHsp cage was determined using absorbance spectroscopy and ranged from 1 to 24 per protein cage depending on reaction conditions (Table 1 and Supporting Information).

Size exclusion chromatography, SDS−PAGE, dynamic light scattering, and transmission electron microscopy were used to characterize the MjHsp protein cages after fluorescein labeling. Size exclusion chromatography showed coelution of the protein cage (280 nm) and fluorescein (500 nm), demonstrating the covalent attachment of fluorescein to the protein cage (Figure 4A). The elution profile of fluorescein

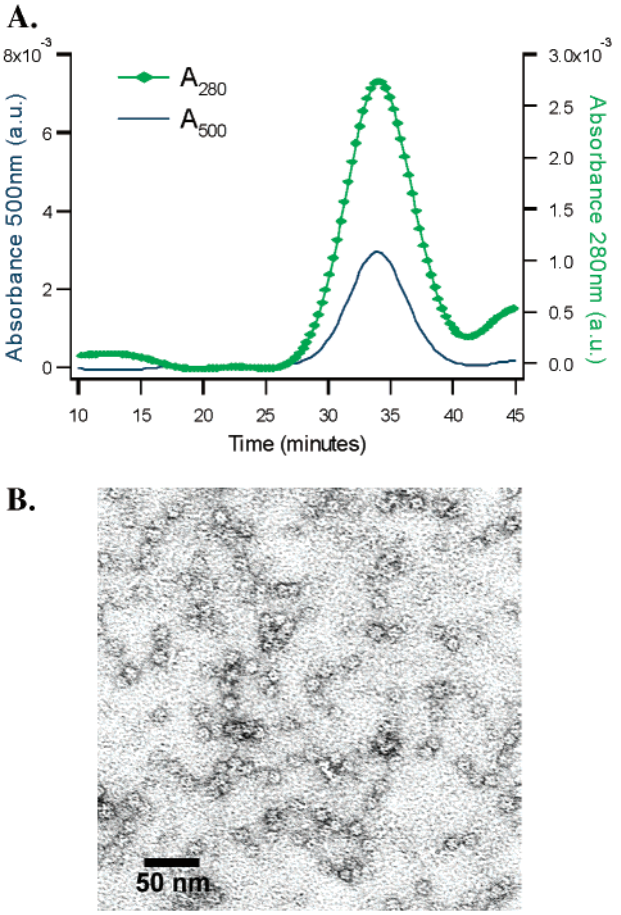

Figure 4. (A) Size exclusion chromatography elution profile of HspG41C reacted with a 10-fold (10×) molar excess of fluorescein-5-maleimide per subunit. The profile illustrates the coelution of fluorescein (A500) and Hsp protein cage (A280). (B) TEM of fluorescein labeled HspG41C cages negatively stained with uranyl acetate.

labeled Hsp cages was identical to the unreacted protein cages (Figure 2A). These results were confirmed by SDS−PAGE, in which the band corresponding to the fluorescein labeled HspG41C co-migrated with the 16.5 kDa MjHsp protein subunit (Supporting Information). In addition, dynamic light scattering and transmission electron microscopy both revealed 12 nm diameter protein cage particles before and after the fluorescein labeling reactions (Figure 4B, Supporting Information).

We investigated the MjHsp cage for its ability to act as a size constrained reaction environment for iron oxide mineralization by analogy to ferritin, which catalyzes the oxidation of Fe(II) to Fe(III), resulting in the spatially constrained mineralization of ferrihydrite (Fe(O)OH).[20] We followed Fe(II) oxidation activity in the presence of MjHsp cages by monitoring the increase in the ligand-to-metal charge transfer (LMCT) absorbance in the visible spectrum at 400 nm. Addition of Fe(II) to G41C and subsequent air oxidation resulted in the formation of a homogeneous rust colored solution. When imaged by TEM, small iron oxide particles were seen with an average diameter of 9 ± 1.2 nm (Figure 5A). Both the wtMjHsp and MjHspG41C cages showed similar mineralization capabilities. The presence of

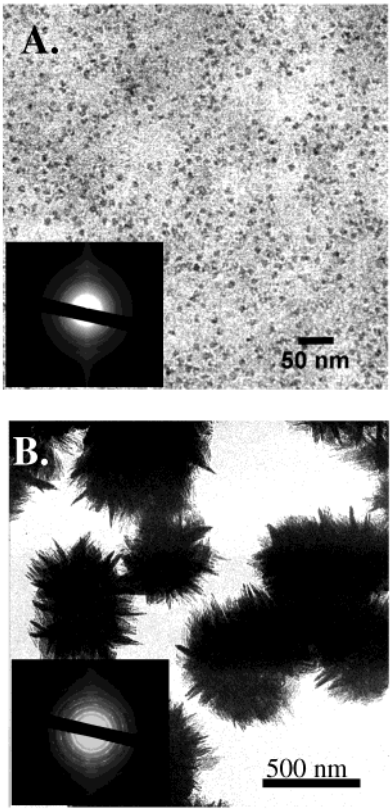

Figure 5. Transmission electron microscope (TEM) images (A) TEM of iron oxide cores inside Hsp cages; 50 nm scale bar. (B) TEM of control sample illustrating the bulk precipitation of iron oxide in the absence of Hsp protein cages; 500 nm scale bar. The insets show the electron diffraction from each sample.

iron in the particle was confirmed by electron energy loss spectroscopy (EELS). In contrast, Fe(II) oxidation in the absence of MjHsp protein cages resulted in rapid bulk precipitation of a ferric oxide due to unconstrained particle growth (Figure 5B). Electron diffraction of the bulk precipitate showed *d*-spacings consistent with the major reflections for lepidocrocite[21] (3.28 Å (120), 2.46 Å (031), 1.93 Å (200), 1.72 Å (151), 1.51 Å (231), 1.39 Å (251)). The electron diffraction from the mineralized MjHsp, however, indicated the presence of a poorly crystalline ferric oxide phase having *d*-spacings consistent with ferrihydrite[22] (2.50 Å (110), 1.93 Å (113), and 1.55 Å (115)). While the high order reflections for ferrihydrite and lepidocrocite are very similar, the absence of large *d*-spacing reflections in the mineralized MjHsp diffraction suggests ferrihydrite rather than lepidocrocite. Clearly, the Hsp protein shell acts as a constrained reaction vessel for spatially selective mineralization of Fe(O)OH. From the crystal structure of the assembled MjHsp, it can be seen that the interior surface of the cage has a slight excess of acidic residues, which we have previous shown to be sufficient to direct oxidative hydrolysis and mineralization of iron oxide.[4,7] As we have shown with other protein cages, this spatially confined mineralization suggests that MjHsp could serve as a template for the synthesis of other mineral phases with magnetic properties important for biomedical[14] and nanoelectronic purposes.

These results demonstrate the versatility of the MjHsp cage as a template for the synthesis of hard (inorganic) or soft (organic) materials. Significantly, the symmetry of the self-assembly architecture affords precise molecular level control over the spatial distribution of attached ligands resulting in an ordered multivalent material. The differences between the interior and exterior surfaces of the Hsp cage have allowed us to direct mineralization reactions in a spatially controlled manner. Currently we are exploring the synthesis and encapsulation of other species as well as the attachment of ligands to develop composite materials with specific biomedical, magnetic, or catalytic properties.

Acknowledgment. The authors thank Zachary Varpness for mass spectroscopy data. This work was funded by grants from NIH (RO1 GM61340, RO1 EB00432) and the National Aeronautics and Space Administration (NAG5-8807).

Supporting Information Available: Additional information, including protocols for gene cloning, protein expression and purification, and PCR mediated site directed mutagenesis; methods for fluorophore labeling and the quantification of the number of fluorophore molecules per protein cage; and supplemental figures illustrating Fl-Mal labeling of HspS121C, dynamic light scattering, mass spectroscopy, and gel electrophoresis data. This material is available free of charge via the Internet at http://pubs.acs.org.

References

(1) *Biomimmetic Materials Chemistry*; Mann, S., Ed.; VCH: New York, 1996.
(2) Whaley, S. R.; English, D. S.; Hu, E. L.; Barbara, P. F.; Belcher, A. M. *Nature* **2000**, *405*, 665−668.
(3) Lee, S. W.; Mao, C., Flynn, C. E., Belcher, A. M. *Science* **2002**, *296*, 892−895.
(4) Allen, M.; Willits, D.; Mosolf, J.; Young, M.; Douglas, T. *Adv. Mater.* **2002**, *14*, 1562−1565.
(5) Douglas, T.; Young, M. *Nature* **1998**, *393*, 152−155.
(6) Douglas, T.; Young, M. *Adv. Mater.* **1999**, *11*, 679−681.
(7) Douglas, T.; Strable, E.; Willits, D.; Aitouchen, A.; Libera, M.; Young, M. *Adv. Mater.* **2002**, *14*, 415−418.
(8) Gilitzer, E.; Willits, D.; Young, M.; Douglas, T. *Chem. Commun.* **2002**, 2390−2391.
(9) Wang, Q.; Lin, T.; Johnson, J. E.; Finn, M. G. *Chem. Biol.* **2002**, *9*, 813−819.
(10) Wang, Q.; Kaltgrad, E.; Lin, T.; Johnson, J. E.; Finn, M. G. *Chem. Biol.* **2002**, *9*, 805−811.
(11) Wang, Q.; Lin, T.; Tang, L.; Johnson, J.; Finn, M. G. *Angew. Chem., Int. Ed.* **2002**, *41*(3), 459−462.
(12) McMillan, R. A.; Paavola, C. D.; Howard, J.; Chan, S. L.; Zaluzec, F. J.; Trent, J. D. *Nature Materials* **2002**, *1*, 247−252.
(13) Kim, I.; Hosein, H.-A.; Strongin, D. R.; Douglas, T. *Chem. Mater.* **2002**, *14*, 4874−4879.
(14) Bulte, J. W. M.; Douglas, T.; Mann, S.; Frankel, R. B.; Moskowitz, B. M.; Brooks, R. A.; Baumgarner, C. D.; Vymazal, J.; Strub, M.-P.; Frank, J. A. *J. Magn. Res. Imag.* **1994**, *4*, 497−505.
(15) Kim, K. K.; Kim, R.; Kim, S. H. *Nature* **1998**, *394*, 595−599.
(16) Kim, K. K.; Yokota, H.; Santoso, S.; Lerner, D.; Kim, R.; Kim, S. H. *J. Struct. Biol.* **1998**, *121*, 76−80.
(17) Kim, R.; Kim, K. K.; Yokota, H.; Kim, S. H. *Proc. Natl. Acad. Sci. U.S.A.* **1998**, *95*, 9129−9133.
(18) Bova, M. P.; Huang, Q.; Ding, L.; Horwitz, J. *J. Biol. Chem.* **2002**, *277*, 38468−38475.
(19) Haughland, R. P. *Handbook of Fluorescent Probes and Research Chemicals*, 6th ed.; Molecular Probes: Eugene, OR, 1996.
(20) Chasteen, N. D.; Harrison, P. M. *J. Struct. Biol.* **1999**, *126*, 182−194.
(21) Lepidocrocite, (γ-FeOOH) JCPDS file 08-0098.
(22) Ferrihydrite ($Fe_5O_7(OH)\cdot 4H_2O$ JCPDS file 29-0712.

NL034786L